LA-UR - 81-2793

CONF-810429--40

Los Alamos National Laboratory is operated by the University of California for the United States Department of Energy under contract W-7405-ENG-36

MASTER

TITLE: A MULTIPLE-POINT THOMSON SCATTERING MEASUREMENT FOR THE ZT-40 REVERSED-FIELD PINCH

AUTHOR(S): K. B. Freese, R. S. Massey, Rita Gribble, and J. D. Smith

SUBMITTED TO: Proceedings of the Los Alamos Conference on Optics '81
Santa Fe, New Mexico

Los Alamos Los Alamos National Laboratory
Los Alamos, New Mexico 87545

FORM NO. 836 R4
ST. NO. 2629 6/81

EAB

A Multiple-Point Thomson Scattering Measurement for the ZT-40 Reversed Field Pinch*

K. B. Freese, R. S. Massey, Rita Gribble, and J. D. Smith

Los Alamos National Laboratory

ABSTRACT

A multiple-point Thomson scattering device, capable of giving radial electron temperature profiles, has been developed for the ZT-40 reversed field pinch experiment. The measurement is accomplished by observing the Thomson scattered spectrum from along an entire chord of focused ruby-laser light traversing the minor diameter of the plasma. A specially built, nearly diffraction limited laser is focused through the plasma using a long focal length lens. The detector uses specially designed collection optics to focus the entire scattering volume into an image dissecting array of fiber optics, which serve as the entrance slit to an anastigmatic spectrograph. The dispersed spectra from all the spatial locations are detected with a gated microchannel plate image intensifier, and recorded on an optical multichannel analyzer using a SIT tube detector. A computer interface is used for data transmission for analysis. Results from the ZT-40 experiment will be presented.

Introduction

During the past 10 years the measurement of plasma electron densities and temperatures by Thomson scattering has become a relatively standard technique in Magnetic Fusion Energy (MFE) research experiments. The data obtained from such measurements have become essential to the understanding of the physics of plasma confinement by magnetic fields. In particular, the evolution of temperature and density distribution in the plasma is required to estimate important parameters such as the energy confinement time for an experiment. Most routine Thomson scattering measurements provide data at only one point in the plasma, at one point in time.[1] Information about the evolution of temperature and density profiles in the plasma has to be compiled from many repeated measurements made at various places in the plasma at many different times during successive plasma discharges. The accuracy of such composite profiles depends on the shot-to-shot reproducibility of the plasma-producing device, and this is often a problem.

To obtain reliable temperature and density profile data for the ZT-40 reversed field pinch (RFP) experiment,[2] we have developed a system to observe, simultaneously, Thomson scattered signals from many points along the incident laser beam as it passes through a diameter of the plasma cross section. The approach taken follows the work first done by Siemon[3] and later by Bretz, et al.[4] The method uses a low-divergence, high-power, Q-switched ruby laser, focused into a long thin scattering volume through the plasma. The scattered light is collected from the entire length of the volume and focused onto a linear fiber-optic array that dissects the image into many discrete spatial segments. The segments are stacked forming the entrance slit of a low-resolution, anastigmatic spectrograph. Since each spatial segment is at a different height in the entrance slit, the output image of the spectrograph is a two-dimensional intensity pattern described by plasma position (spatial segment) along the ordinate and wavelength along the abscissa. This intensity pattern is focused onto a gated microchannel plate intensifier that forms the first stage of an intensified vidicon image digitizer. This technique provides instantaneous profile data for electron temperature and density in the plasma; time-evolution of the profiles still must be compiled from many measurements made at different times during reproducible plasma discharges.

In this paper, we report the design and development of our apparatus and present preliminary results from measurements made on the ZT-40 RFP experiment.

Background

Our system was designed to measure electron temperatures between 5 and 500 eV, at electron densities near 10^{14} cm^{-3}. Under these conditions and for a ruby laser source (λ = 6943 Å), the plasma electrons should scatter the incident light as independent radiators having total Thomson cross section[5]

*Work performed under the auspices of the U. S Department of Energy.

$$\sigma_T = \frac{8\pi}{3} r_o^2 \quad , \tag{1}$$

where $r_o \equiv e^2/m_e c^2 = 2.82\times10^{-13}$ cm is the classical electron radius. For a thermal distribution of electron speeds, the scattered light is spread in wavelength, having a spectrum that reflects the gaussian distribution function of the scattering electrons. The differential number of scattered photons can be expressed as a function of the scattered wavelength, λ_s, as[5]

$$N_p(\lambda_s)\, d\Omega\, d\lambda_s = \frac{N_I n_e r_o^2 L\, d\Omega\, d\lambda_s}{\lambda_i\, \delta\, \pi^{1/2}} \exp\left[-\frac{(\lambda_s - \lambda_i)^2}{\lambda_i^2\, \delta^2}\right] \quad , \tag{2}$$

where N_I = number of incident photons
n_e = electron density
r_o = classical electron radius
L = length of scattering volume observed
Ω = observation solid angle
λ_i, λ_s = incident and scattered wavelengths
$\delta = [8kT_e/mc^2]^{1/2} \sin\theta_s/2$
k = Boltzman's constant
T_e = electron temperature
m = electron mass
c = speed of light
θ_s = angle between incident and scattered photons.

The number of photoelectrons produced at each channel of a multichannel spectral detector can be estimated as,

$$N_{pe} = N_p\, \eta T\big|_{\lambda_{ch}}\, \Delta\lambda\, \Delta\Omega \quad , \tag{3}$$

where λ_{ch} = mean wavelength for each channel
η = quantum efficiency of detector
T = spectral transmission function of the optical train
$\Delta\lambda$ = spectral width of channel
$\Delta\Omega$ = observation solid angle

For the conditions expected in ZT-40 ($n_e = 10^{14}$ cm^{-3}, $T_e = 100$ eV) and for the parameters of our instrument,

$N_I = 3.5\times10^{19}$ (10 J)
$\Delta\Omega = .022$ sr
$\Delta\lambda = 30\text{A} = 3\times10^{-7}$ cm
$\eta = .06$
$T = .01$
$L = 1$ cm
$\theta_s = 90^\circ$

we estimate the number of detected photoelectrons in any channel to be

$$N_{pe} = 316 \exp\left[-\frac{(\lambda_{ch} - \lambda_i)^2}{(196\text{A})^2}\right] \quad , \tag{4}$$

where wavelengths have been expressed in angstroms. Integrating over all wavelengths detected ($\lambda \leq 6940$ A), each spatial segment should produce approximately 2000 photoelectrons. This number is large enough to give good statistics if the plasma background radiation does not swamp the signal. An estimate of the ratio of total detected scattered photons to the number of detected bremsstrahlung photons in the same spectral region can be given by[6]

$$\frac{N_{ts}}{N_{brem}} = \frac{4\pi E_i r_o^2 \lambda_i^2 L}{t_i (7.94\times10^{-40}) n_e V_p} \quad , \tag{5}$$

where E_i = energy in incident laser beam
t_I = integration time for the gated detector (usually t_I = pulse width of laser)
V_p = effective volume of plasma seen by detector

and r_o, λ_i, L, n_e are as defined previously. For expected conditions, $n_e = 10^{14}$ cm^{-3}, E_i = 10 J, t_I = 100 ns, and V_p = 8 cm^3, Eq. (5) yields

$$\frac{N_{ts}}{N_{brem}} = 750 \quad , \tag{6}$$

which should give a comfortable margin for signal-to-noise ratio. However, bremsstrahlung is only a lower bound to the intensity of the background plasma light. In practice, the background intensity is usually much higher, and, in the case of ZT-40, the background light in the spectral region of interest was over a thousand times bremsstrahlung. This was due to the presence of impurity ion line radiation.

System Description

A schematic diagram of the entire system is shown in Fig. 1. A low-divergence, high-power ruby laser beam is focused to a thin waist passing through the 40-cm diameter of the ZT-40 discharge vessel. The scattered light is collected from every point along the beam by a specially designed, large-aperture, wide-angle lens attached to one of the 50-mm diameter, sapphire viewing windows in the side of the ceramic vessel. The image of the scattering volume is focused onto an array of light guides that relay the signal to a simple grating spectrograph. A gated detector integrates the resulting spectral information and a digital television camera acquires the image for further analysis. Each part of the system is described in detail in the following subsections and is summarized in Table I.

The Laser

The laser is a Q-switched, ruby system capable of delivering a 10-J, 20-ns FWHM pulse having < 0.25-mrad divergence at 19-mm beam diameter. The system was built on an optical table (NRC) from standard Korad parts and commercially available lenses and mirrors. The low divergence is achieved by low-order mode selection in the oscillator and subsequent amplification.

The oscillator consists of a 4-inch holographic-quality ruby laser head in a flat-flat cavity having an internal converging lens. The ratio of cavity length to lens focal length was chosen to produce near-confocal oscillator conditions.[7] In addition, an internal aperture is used to further reduce high-order transverse modes. The resultant mode structure of the oscillator beam is a combination of TEM_{00} and TEM_{01}, with TEM_{01} being the dominant mode. The beam diameter is approximately 3 mm.

The output from the oscillator is expanded to 10 mm, using a Fourier transform telescope and spatial filter. The expanded beam is amplified through two 4-inch ruby rods and is expanded again to 19 mm using a simple Galilean telescope. The beam passes through the final amplifier which consists of 14-inches of ruby rod (an 8-inch plus a 6-inch head). The collimated output beam travels approximately 12 meters before it is focused into the ZT-40 plasma. The laser operates reliably and remains stable over several months.

Beam Delivery System

The rejection ratio for unshifted stray laser light for the grating spectrograph is only ~ 10^4, and any significant stray reflection of the incident laser beam entering the spectrograph would swamp the small Thomson scattering signal, which is approximately 10^{14} times less intense than the incident laser beam. So care must be taken to insure that the laser passes through the plasma without hitting any of the apertures along the way. Furthermore, small-angle scattering off optical elements in the beam path create a beam halo which must also be prohibited from striking the interior of ZT-40 walls and reflecting into the spectrograph. To accomplish this goal, the beam delivery optics, vacuum windows, beam apertures and baffles had to be carefully designed. The problem was made more difficult because the wall material inside ZT-40 was highly-reflective white ceramic and no viewing dumps (black background for the objective scene) were permitted inside ZT-40.

TABLE I. ZT-40 MULTIPLE-POINT THOMSON SCATTERING PERFORMANCE SPECIFICATIONS

Ruby Laser	
Total ruby length	60 cm
Output beam diameter	19 mm
Beam divergence	<0.25 mrad
Pulse width	30 ns
Energy/pulse	~10 J
Focus lens	2 m efl
Focus spot	<.5 mm
Hemi-Concentric Achromatic Objective	
EFL	86 mm
f/#	2.4
Full field	90°
Magnification	2:1
Fiber-Optic Image Dissector	
Number of elements	36
Eleme [illegible]ze	2 mm×4 mm
Spectrograph	
EFL	0.6 m
f/#	6.0
Grating	1800 ℓ/mm holographic
Slit	4 mm×72 mm - compound curve
Resolution at image	~1 mm max = 8 Å
Resolution with slit	~30 Å
Detector Stage	
Reduction lens 6:1	120 mm f/1.0
MCP intensifier	18 mm S-20R/P-20 (ITT 4111)
Relay lens 1:1	2-50 mm f/0.75
Detector	OMA II SIT tube or ISIT tube
MCP gate	100 ns
Scan Pattern	16 tracks (over 32 spatial elements×500 channels/tracks 'scan

The entrance and exit vacuum windows are 2 m and 1 m, respectively, from the laser focal point. They are made from highly polished, high-purity fused silica, mounted at Brewster's angle, and because the peak surface power density of the laser is quite high (GW/cm^2), the windows have to be kept scrupulously clean.

The key elements in reducing stray light are specially designed baffles and halo dumps (Fig. 2) in both entrance and exit beam tubes. The halo dumps are nested, long cylinders, concentric to the beam path. The ends of the cylinders toward the plasma are razor-edged and all surfaces are shiny black (black chrome). Their function is to absorb via multiple, shallow-angle reflections the halo surrounding the beam that enters the plasma region. Their effectiveness is proved by a residual stray laser light level in the detector, equivalent to a Thomson scattering signal from a 7×10^{15} cm^{-3} density plasma. This signal is easily masked in the spectrograph, which should permit measurements of Thomson scattering from electron densities down to ~ 10^{12} cm^{-3}. The success of the entire beam delivery system is enhanced by the extremely low divergence of the laser beam.

Collection Optics

The design of the optical train, including the grating spectrograph, required a systems approach made possible by the availability of the ACCOS V optical design code. The first element in the train was the wide-angle objective. It had to collect the scattered signal within a 90° field of view at the largest possible solid angle. By using fiber optics at the image surface, a highly curved image field was permitted, greatly simplifying the design. Another constraint on the lens was that it had to be as close to the sapphire viewing window as possible to avoid vignetting at the extremes of the field. The solution chosen was a cemented doublet, hemi-concentric achromat (Fig. 3). The lens was designed with a plano front surface that could optically contact the viewing window and provide maximum aperture. However, since no rigid mechanical connections were permitted between the ceramic torus and the outside world (the torus was free to move ± 1 mm to accommodate contraction while under vacuum), the lens had to be mounted on a sliding, spring-tension support that held the lens in optical contact with the sapphire window. The fiber-optic

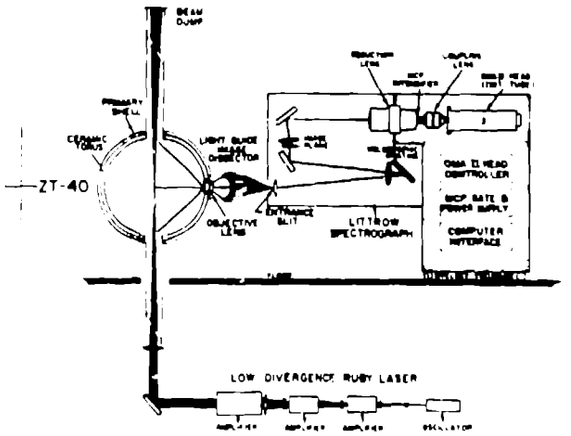

Fig. 1. A schematic diagram showing the layout of the multiple-point Thomson scattering measurement apparatus for ZT-4C.

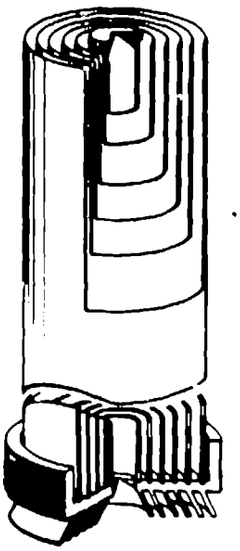

Fig. 2. A cut-away view of the halo dump used to absorb stray light that is non-parallel to the incident laser beam.

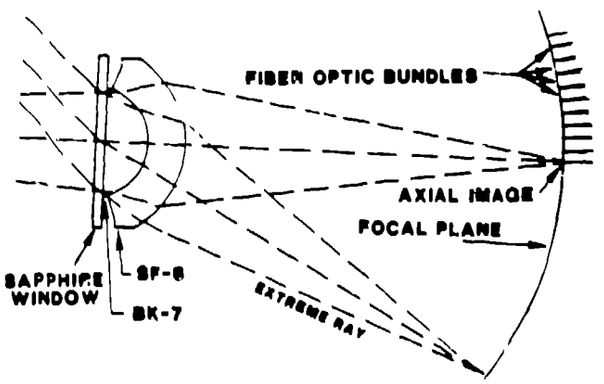

Fig. 3. A ray-trace diagram of the hemi-concentric achromat objective lens showing the highly curved image surface.

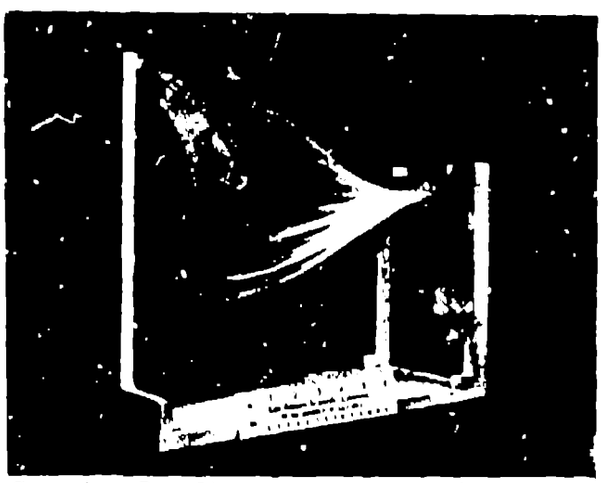

Fig. 4. The fiber optic image dissector that relays the curved objective image to the compound-curved entrance slit of the spectrograph.

image dissector was conveniently mounted on this structure also which helped maintain alignment once proper focus had been established.

The image dissector, shown in Fig. 4, relayed the image to the spectrograph slit and reshaped the aspect ratio of the image. The fiber-optic array at the image formed by the objective lens comprised 36 bundles, each 2-mm wide by 4-mm high, stacked end-to-end. When entering the spectrograph slit, the bundles were stacked side-by-side. Thus, the 144-mm·2-mm objective image was converted to a 72-mm×4-mm entrance slit. The use of fiber optics also permitted a simple way to reduce some of the aberrations of the spectrograph. The field curvature of the spectrograph image could be flattened in one dimension by stacking the input fibers along a curve concave toward the grating. The usual curved slit image of grating spectrographs[8] could be straightened by bending the slit perpendicular to

the optical path. Thus, a compound-curved entrance slit held the fiber bundles in the correct positions to give a fairly flat (one dimension of field curvature cannot be removed), rectiliniar image.

This flexible arrangement permitted rapid modification of the image presented to the spectrograph. Some of the spatial-segment bundles were moved off the line image of the scattering volume, and used to measure background light from similar volumes adjacent to the laser path. The signals from these segments were subtracted from the adjacent data channels to compensate for background light.

The Spectrograph

The spectrograph had a simple Littrow design, employing commercially available telescope lenses and a holographic grating. The spectrograph provided an 8 Å/mm dispersion at the image. Because our resolution element for this measurement was quite large at the detector (~ 30 Å), the absolute resolution of the spectrograph could be relatively poor, having an image spot size of ~ 1 mm.

The Detector

The output image of the spectrograph is approximately 72 mm × 72 mm and must be reduced to fill the photo-cathode of an 18-mm microchannel plate (MCP) image intensifier (ITT 4111). A commercially available, Zeiss R-Biotar (120 mm, f/1.0) serves the purpose. The MCP intensifier provides the first stage of optical gain and the gated photocathode serves as a fast optical shutter. The gate period is ~ 100 ns. Two KOWA, 50-mm, f/0.75 lenses relay the intensified image at 85% transmission from the MCP tube to the faceplate of an OMA II, Model 1256 detector head. The OMA II (Optical Multichannel Analyzer) is a versatile, digital, television system built by Princeton Applied Research. These elements, shown schematically in Fig. 5, are mounted on a sliding optical rail assembly that allows adjustment of each element individually, and a sliding adjustment of the entire assembly to achieve best focus of the spectrograph image.

Detector Development

The detector system, which includes the MCP and OMA II, is remotely controlled and interrogated by the ZT-40 control computer. A schematic is given in Fig. 6. The integration of these various components into a working system required a considerable amount of circuit design and fabrication.

The MCP shutter operates in 3 modes: a) fast gating (~ 100 ns) synchronized with the laser monitor pulse, b) a longer gate pulse of ~ 10 μs useful for some of the calibration

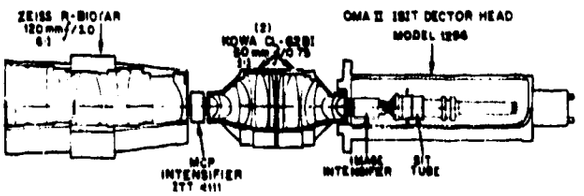

Fig. 5. The spectrograph image detector assembly, showing the reduction lens, microchannel plate intensifier, relay lenses, and digital TV head.

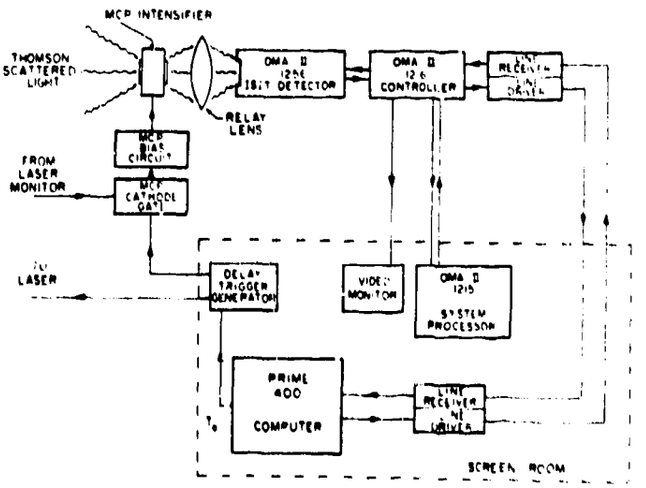

Fig. 6. A schematic diagram of the computer control system for the multiple-point Thomson scattering measurement apparatus.

procedures, and c) a continuously open 'focus' mode for adjustments of the entire system in very subdued light.

Since the OMA II needs to operate in a continuous scan mode, it requires that the ZT-40 bank be fired only during the time window between frames.

It is an intrinsic property of the SIT tube that several scans must be made to obtain all the available signal. The scan pattern can be varied by the operator. A typical scan will generate approximately 8000 16-bit words of data, requiring an 8K×16-bit capacity memory buffer. This is available in a CAMAC module (not shown in Fig. 6). Not atypical of the entire project was the discovery and cure of a design flaw in the memory buffer, of which the vendor was unaware.

A triple-wall nested magnetic shield (two layers of 18 gauge Mu-metal and an inner wrap of Conetic foil) protects the detector electronics from the ~ 100 gauss stray fields that were found to exist in the vicinity of ZT-40 during machine operation.

Results

Without the laser, the apparatus functioned as a low-resolution, but very high-sensitivity spectrograph. A systematic study of the background spectra revealed that the background light was dominated by impurity atomic spectra. Furthermore, the correlation between signals from adjacent spatial segments was not consistent shot-to-shot which meant that subtraction of the background signals would be difficult. Preliminary identification of some of the observed spectral lines showed low-level ionization of wall impurities (oxygen, silicon) and wall-embedded gasses (nitrogen), that suggested that the background light may have come from wall-plasma interactions near the viewing window. Later, this idea was supported by a post-mortem of the ceramic torus that showed considerable discoloration of the windows and scorching of the ceramic walls.

These problems made detection of the Thomson-scattered signal difficult. The sensitivity of the instrument was calibrated by Rayleigh scattering from low-pressure (1 to 7 psi) fills of nitrogen. The calibration revealed that the background light was ~ 4 times larger than the expected Thomson scattering signal, or ~ 3000 times the classical bremsstrahlung level.

Figure 7 shows the data for fifteen tracks (spatial segments) of plasma background light. Under the intensity surface spanned by track number and wavelength, is drawn a typical Thomson-scattered signal for one track, to show the relative sizes of the signals. The large background level prevented us from measuring plasma temperature except for high-density, low-temperature conditions (see Fig. 8) where the signals were large enough to be measured. Measurement of smaller signals required increased sensitivity, but saturation of the detector by the background signal made such measurements impossible.

Conclusions

The multiple-point Thomson scattering measurement was designed, built, and tested on the ZT-40 reversed field pinch experiment. The apparatus performed as expected, but unexpectedly large levels of impurity radiation from plasma-wall interactions dominated the measurement, limiting the usefulness of the device to high-density, low-temperature plasma measurements.

ZT-40 was modified to use a metallic (inconel) vacuum vessel instead of the one made of ceramic. Preliminary results from the new ZT-40M (M for metallic) indicate that background light will be significantly (10 to 100 times) reduced, allowing us to measure plasma temperatures and densities under more interesting and relevant conditions, i.e., low density and high temperature.

Acknowledgments

The authors would like to acknowledge the assistance and support of Richard Siemon who was instrumental in starting this project and Richard Bartch who supervised the design and construction of the low-divergence laser. Our appreciation goes to Dick Hicks, Ed Mignardot, and Di Ortega for assembly of many parts and subsystems used in the project, and to the plasma diagnostic staff of Princeton Plasma Physics Laboratory for many helpful discussions, suggestions, and designs.

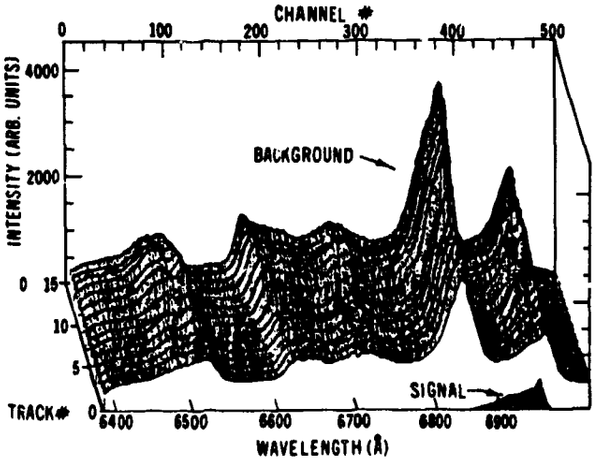

Fig. 7. A 3-D perspective plot of the background light intensity pattern observed for one discharge in ZT-40. Masks in the spectrograph for $\lambda > 6943$Å and at 6562Å ± 50Å (H_α) appear as flat valleys in the plotted intensity surface.

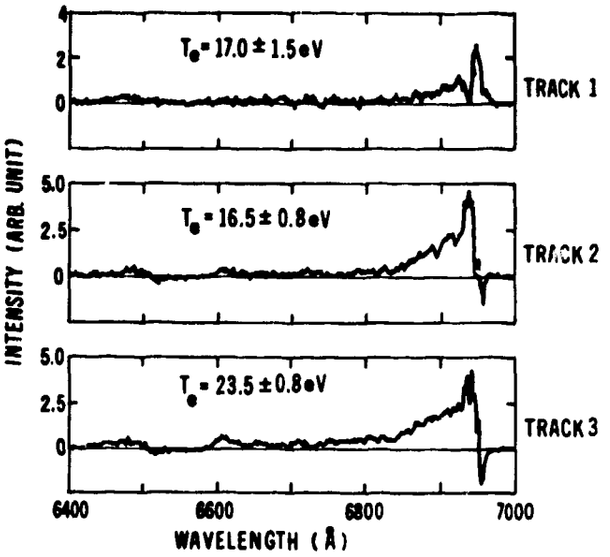

Fig. 8. Analyzed Thomson scattering signals for three typical tracks (spatial segment in the ZT-40 plasma. Plasma density for these data was approximately 1.4×10^{15}cm^{-3}. The temperatures are inferred by least squares fitting the theoretically predicted spectrum to the data, where temperature is one of the fit parameters.

References

1. A. W. DeSilva and G. C. Goldenbaum, in Methods of Experimental Physics, H. R. Griem and R. H. Lovberg, Eds. (Academic Press, New York, 1970), Vol. 9A, p. 213.

2. D. A. Baker, et al., "Initial Reversed-Field Pinch Experiments on ZT-40 and Recent Advances in RFP Theory," Proc. 8th Int. Conf. on Plasma Phys. and Contr. Nucl. Fusion Res. (IAEA, Vienna, 1981) Vol. 2, paper L-2-7.

3. R. E. Siemon, et al., in "LASL Controlled Thermonuclear Research Program," K. S. Thomas, Compiler, (Los Alamos Scientific Laboratory, 1978) Progress Report, LA-7082-PR, pp. 127-133.

4. N. Bretz, D. Dimock, V. Foote, D. Johnson, D. Long, and E. Tolnas, "Multichannel Thomson Scattering Apparatus," Appl. Opt. 17, p. 192 (1978).

5. J. Sheffield, Plasma Scattering of Electromagnetic Radiation, (Academic Press, New York, 1975), p. 44.

6. Ibid., p. 70.

7. W. K. Koechner, Solid-State Laser Engineering, (Springer-Verlag, New York, 1976), Chap. 5.

8. J. F. James and R. S. Sternberg, The Design of Optical Spectrometers, (Chapman and Hall, London, 1969), Chap. 5.